PROC. OF JSCE,
No. 197, Jan. 1972

THE EFFECT OF END RESTRAINT CONDITION ON THE FRACTURE MECHANISM AND STRENGTH OF ROCK-LIKE MATERIALS IN COMPRESSION

By Koji NAKAGAWA, Shoichi KOBAYASHI** and Yoshiji NIWA****

1. INTRODUCTION

The uniaxial compressive strength of rock-like materials such as mortar, concrete, rock is of a fundamental prerequisit for structural designs. Knowledge of the real strength and the real fracture mechanism under uniaxial compression are also important to make clear failure condition and failure mechanism under multiaxialstresses.

In usual compression test of rock-like materials the lateral deformation of the end of specimen is restrained by the loading platen and the deformation can not become homogenious throughout the specimen, because Young's modulus and Poisson's ratio of the specimen are different from those of the loading platen (generally, the ratio of Poisson's ratio to Young's modulus of the specimen ν_s/E_s is larger than that of the loading platen ν_p/E_p). Thus, the apparent uniaxial compressive strength are somewhat different from the real one, as reported by many investigators.

An approach to reducing the end friction by using lubricating materials between the specimen end and the loading platens attempted by many investigators. However, the effects of these lubricating materials are not equal when elastic properties of the specimens and loading platen are different each other. Moreover, the effects may change with the change of the mechanical properties of the specimen during the failure process. The numerical estimation of the effect of lubricating material is not so easy. There is an effort to produce a uniform stress distribution in a potential region of failure by reducing the sectional area in the effective part of the specimen. However, it is not convenient to make such specimen.

On the other hand, there is a direction of study in which one examines the end restraining effect on the strength and the fracture mechanism of the specimen and estimates the real uniaxial compressive testing state. There are several stress analyses by the use of theory of elasticity and the finite element method. The effects of the finite end friction on the stress state are also analysed. These analyses are, however, valid only when the specimen is perfectly elastic, and they introduce some errors if the mechanical properties of the material are not uniform throughout the specimen with the progress of failure.

In the present paper, the authors analysed the failure process of cylindrical specimens with several height-to-diameter ratios under several end-lubricating conditions. The progressive failure condition was used in the finite element analysis. The analysed results are compared with the reported uniaxial compression test results and the effects of end frictions on the strength and fracture mechanism of uniaxially compressed rock-like materials were discussed.

2. NUMERICAL ANALYSIS

In the present study, a cylindrical specimen of mortar is analysed for a model. The properties of the mortar is such that as made with a mix ratio Normal Portland cement : Toyoura sand : Water= 1.0 : 2.0 : 0.6 by weight and was cured in 20°C water bath for four weeks.[1)]

In the present finite element analysis, the individual element was assumed to behave isotropically in the each stress state.

(1) Failure condition

In numerical analysis, it is of fundamental importance to choose the appropriate failure condition

* Assistant, Department of Civil Engineering, Kyoto University
** Assistant Professor, Department of Civil Engineering, Kyoto University
*** Professor, Department of Civil Engineering, Kyoto University

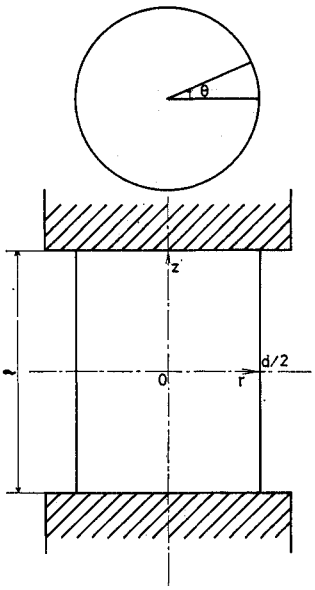

Fig. 1 Cylindrical specimen and cylindrical coordinates.

of the material. Several failure conditions for mortar and concrete are proposed and some of them are explained in the microscopic point of view. In the present study the phenomenological condition as fit for the model as possible was adopted, because the purpose of the present study is to analyse the effect of end restraint on the strength and fracture mechanism of the specimen when the individual element is supposed to behave macroscopically.

The stress state of the individual element of the specimen is approximately the so-called compressive ($\sigma_1 \geqq \sigma_2 = \sigma_3$) with small confining pressure, save for a few elements. Thus, it is sufficient to take the compressive part of the Rendulic stress curve as a failure condition. The condition was approximated by three straight lines as follows :

$$\sigma_1 = 8\,\sigma_3 + \sigma_0 \qquad \sigma_3/\sigma_1 \leqq 1/28$$
$$\sigma_1 = 4\,\sigma_3 + 1.2\,\sigma_0 \qquad 1/28 \leqq \sigma_3/\sigma_1 \leqq 1/10$$
$$\sigma_1 = 2.5\,\sigma_3 + 1.5\,\sigma_0 \qquad 1/10 \leqq \sigma_3/\sigma_1,$$

where σ_0 is the unixial compressive strength.

In general, the minimum principal stress may be different from the intermediate one in the element. However, the difference between them is small enough in comparison with the maximum principal stress so as to assume the intermediate stress to be equal to the minimum stress. The error introduced by this assumption may be estimated to be negligibly small judged from the shape of the failure surface. In the tension-compression part, the failure condition was extrapolated.

As is well known, mortar and concrete specimen proceed to the ultimate failure or collapse after the complicated history of the progressive failure. The initial fracture surface is a small surface containing the origin[2]. From the macroscopic point of view the material may be assumed to be liner below the stress state about 65% of strength failure, because the amount of fracture at this state is negligibly small compared with the total amount of fracture at strength failure. The discontinuity at which the material reveals non-linear behavior is investigated by Vile[3] and McCreath et al..[4] Niwa et al.[5] also showed the fracture initiation surface in stress spa-

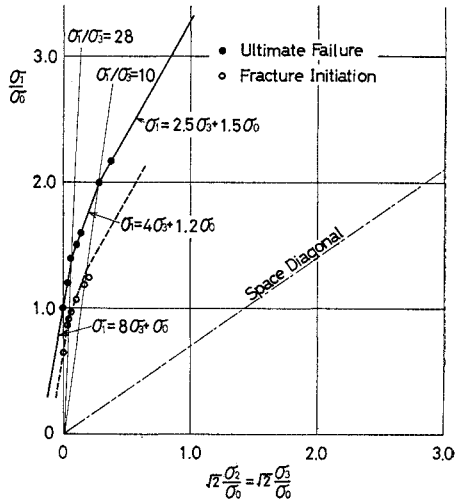

Fig. 2 Experimental results of ultimate failure and fracture initiation by Niwa et al. and assumed criterion lines (σ_0 : uniaxial compressive strength of the material).

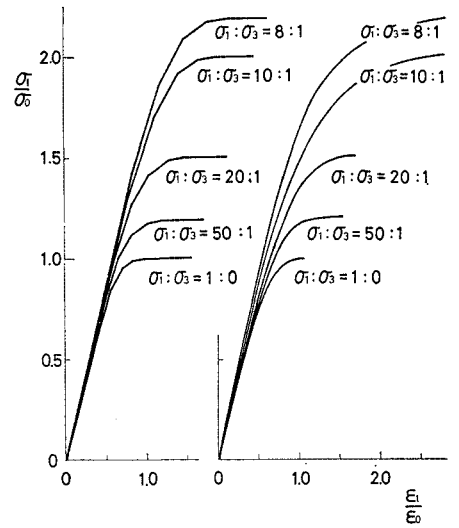

Fig. 3 Experimental and assumed stress-strain curves (ε_0 : axial strain at the strength failure in uniaxially compressed material).

ce. The fracture in the specimen and macroscopic inelastic behavior of the specimen becomes dominant as the stress goes beyond these stress state.

In the present study, in order to show this failure process four isotropically reduced surfaces weremade inside of the strength failure surface and the strss space was divided into six regions (grade of fracture 0～5 : grade 5 indicates ultimately fractured state). Their ratios to the strength failure surface are 0.65, 0.85, 0.95 and 0.99, respectively. The ultimate failure and fracture initiation conditions by Niwa et al. and assumed conditions are shown on the Rendulic stress plane (Fig. 2).

(2) Poisson's ratio and Young's modulus

Poisson's ratios and Young's moduli in the six regions were chosen respectively so as to follow the experimental results of the model material. Fig. 3 shows the experimental and the assumed stress-strain curves, respectively. Fig. 4 shows the increase of the assumed Poisson's ratio with stress.

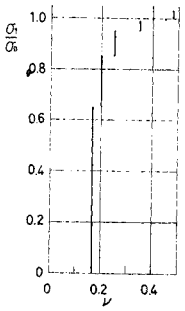

Fig. 4 Increase of Poisson's ratio assumed in calculation.

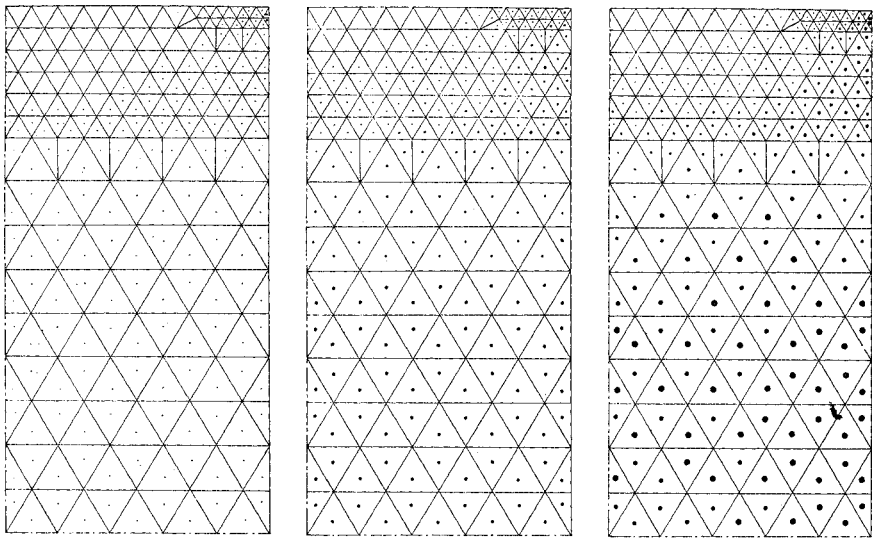

a) $1/d=2.0$ with fixed end $\delta/\delta_0=17/32,\ 22/32,\ 27/37$

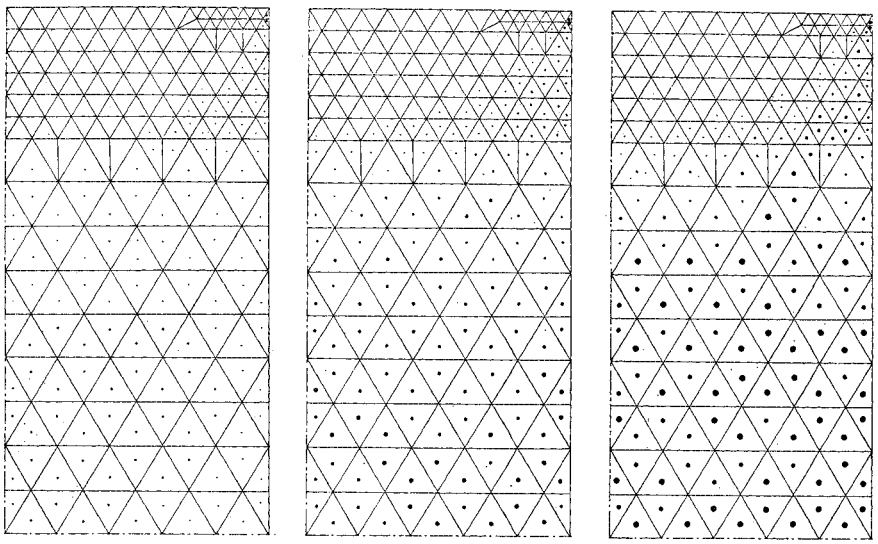

b) $1/d=2.0$ with $\mu=0.05$ $\delta/\delta_0=17/32,\ 22/32,\ 27/32$

Fig. 5 Progressive failure patterns of specimens with increasing end displacement (δ_0 : end displacement at strength failure in ideally uniaxially compressed specimen).

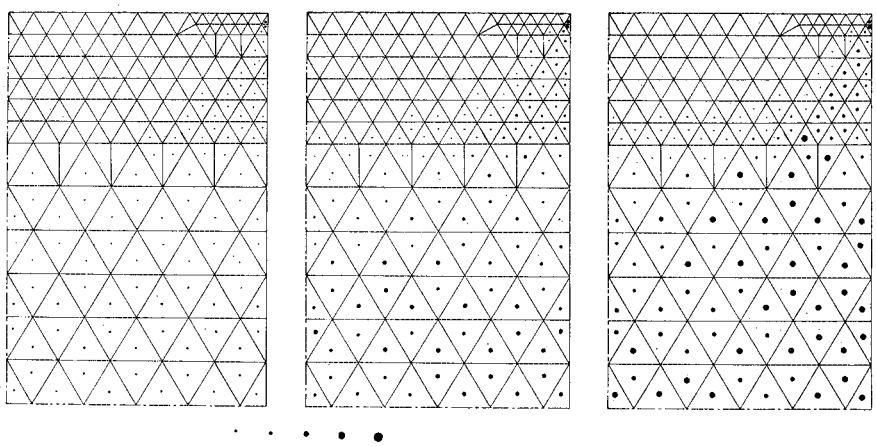

$1/d=1.5$ with fixed end $\delta/\delta_0=17/32,\ 22/32,\ 27/32$

Fig. 6 Progressive failure patterns of specimens with increasing end displacement (δ_0 : end displacement at strength failure in ideally uniaxially compressed specimen).

(3) Iterative procedure

Successive procedure with successively modified elastic constants is carried out. In each step, the stress state of individual element is obtained by successive over relaxation method and examined at what stage it lies on the condition. If the state of stress of the element exceed a certain condition, in the next step new elastic constants are adopted. The error by this calculation is made small enough by taking a small amount of modification of elastic constants.

The axial displacement in each step is 1/32 of the tatal displacement which is given at strength failure in ideal uniaxial compression test.

(4) End restraint and the coefficient of end friction

The end restraint of the specimen with rigid loading platen is controlled by the coefficient of friction between them. The coefficient of end friction in statical mechanics was employed.[6] Strictly speaking, the coefficient of friction may vary as the axial load increases and the initial irregularities of the end surface are gradually smoothed out. In the present study, the coefficient of friction is assumed to be constant irrespective to the normal stress for the sake of simplicity. The efficiency of the law of friction in statical mechanics in the compression test of mortar specimen is verified by Niwa and Kobayashi.[7]

3. RESULTS AND DISCUSSIONS

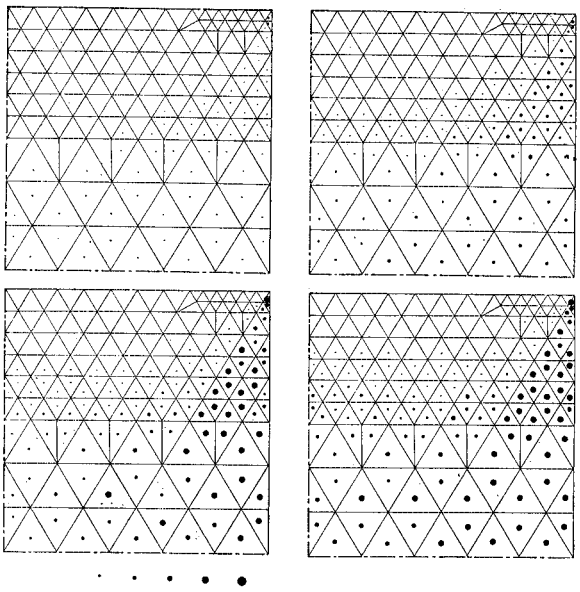

Fig. 7 Progressive failure patterns of specimens with increasing end displacement (δ_0 : end displacement at strength failure in ideally uniaxially compressed specimen).
$1/d=1.0$ with fixed end
$\delta/\delta_0=17/32,\ 22/32,\ 27/32,\ 37/32.$

(1) Progressive failure of specimens

Progressive failure patterns of specimens with increasing end displacements are shown in Figs. 5～7 (in the figures, the grade of fracture of each element is illustrated by the size of solid circle with associated number. Grade 5 indicates ultimately

fractured state). When the height-to-diameter ratio of the specimen is 2.0 and specimen ends are fixed, fracture initiates in the inner part in the central section of the specimen and it grows to the outer part. In the central region the fracture advances very rapidly. The stage of progressive failure is almost equal in each element in this region. Fracture does not initiate near the specimen end exept at the corner. This non-fractured region reduces slightly in size with the increase of the end displacement. The intermediate region between central and non-fractured parts is occupied by the gradually fractured regions.

The smaller the coefficient of end friction becomes, the more uniform mode of fracture is observed. With the coefficient of end friction $\mu=0.05$, each element in the central half-height region is homogeneously fractured before the load becomes almost of the strength failure. The small non-fractured region remains only near the specimen axis at the ends. The grade of fracture becomes higher with the increase of the distance from the specimen ends. In the case of $1/d=1.5$, the fracture patterns are slightly different from those with $1/d=2.0$. When the ends are fixed, fracture initiates almost equal stage in the central region. With the increase of the end displacement, fracture becomes dominant in the outer part of the central region and grows into inner and close-to-end regions. The ultimate fracture is realized at first in the outer part of the central half region of the specimen. It is seen from the figures that the shape of non-fractured region changes very little with the specimen height, and the fracture pattern is determined by the decrease of the region free from the end restraint.

With the coefficient of end friction $\mu=0.05$, the progress of failure becomes considerably uniform and the non-fractured region becomes very small.

In the case of $1/d=1.0$ the non-fractured region is also observed near the fixed ends, and this region decreases considerably in size with the progress of failure of the specimen. The severely fractured region at the corner of the specimen grows with the increase of end displacement, and finally the upper and the lower ultimately fractured regions come to join each other. In short specimens, the mode of fracture is different in the inner and

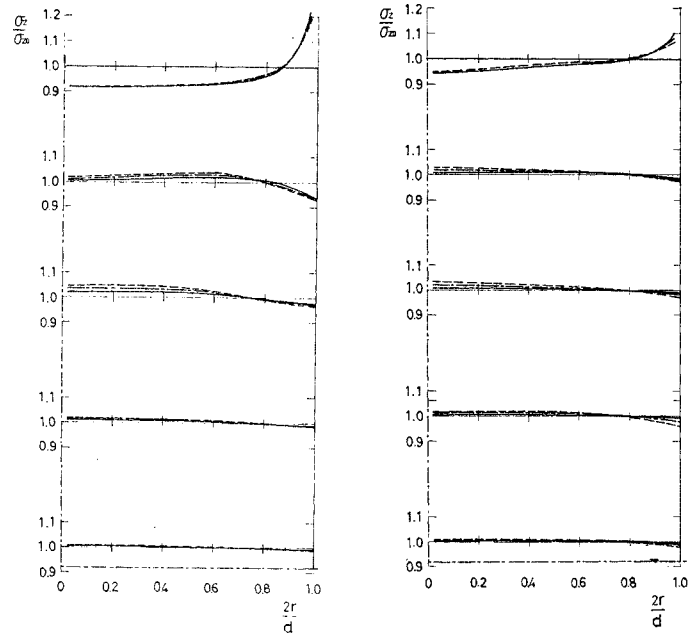

a) $1/d=2.0$ with fixed end b) $1/d=2.0$ with $\mu=0.05$

——— elastic —·—·— $\delta/\delta_0=22/32$ – – – – $\delta/\delta_0=27/32$

Fig. 8 Axial stress distributions at each stage of end displacement.

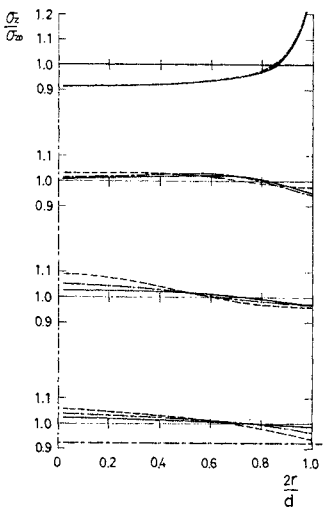

$1/d=1.5$ with fixed end

——— elastic —·—·— $\delta/\delta_0=22/32$

– – – – $\delta/\delta_0=27/32$

Fig. 9 Axial stress distributions at each stage of end displacement.

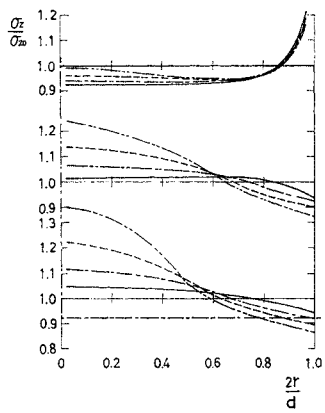

$1/d=1.0$ wits fixed end

——— elastic

—·—·— $\delta/\delta_0=22/32$

– – – $\delta/\delta_0=27/32$

—···— $\delta/\delta_0=37/32$

Fig. 10 Axial stress distributions at each stage of end displacement

the outer parts of the specimen even at the central section. This is the main reason why the fracture modes are not the same in the long and the short specimens. It also explains the cone type failure in the uniaxial compression test of short specimen with no lubricant. (The coefficient of the end friction without lubricant is reported as 0.45～0.65, and the condition can be thought almost equal to the end fixed condition from the previous results.) When the coefficient of end friction μ=0.05, the mode of failure are different from that with fixed end, and it seems considerably uniform at the central section. At the ultimate state the non-fractured regions near the specimen ends almost diminishes and almost all elements are fractured.

(2) The progressive stress distribution

The stress distribution in the elastic cylindrical specimen compressed between rigid platens with various coefficients of end friction were previously reported in detail.[6] The stress state in the specimen changes gradually with the changes of the elastic constants in parts of the specimen. In order to show the changes of stress distribution, the normalized axial stress distributions (σ_z/σ_{z0}) in each height and at each end displacement are shown in Figs. 8～10 (σ_{z0} : average axial stress). When $1/d$= 2.0, the distribution of σ_z does not change remarkably with the progress of failure. The changes of the stress distribution are small and the elastic stress distributions almost reserved during the failure process. Although the difference of the stress between the individual elements at the central section grows with the progress of failure, the stress distribution in the specimen is regarded as considerably uniform the macroscopic point of view.

When $1/d$=1.5, the change of axial stress distribution with the progress of failure becomes remarkabl. Apart from the specimen end, the value of σ_z/σ_{z0} in the inner part is higher than that of in the outer part at the same section because of the end restraint. This tendency becomes larger with the progress of failure of the specimen. The tendency diminishes with the decrease of the coefficient of end friction, and the stress distribution becomes considerably uniform.

When $1/d$=1.0, the axial stress σ_z/σ_{z0} is higher remarkably in the inner part of the specimen than that in the outer part at first. The progress of failure is faster in the outer part than in the inner part of the specimen. With the progress of failure, the axial stress becomes larger in the inner part and smaller in the outer part. The change of stress distribution according to progress of failure reduces with the decrease of the coefficient of end friction μ. However, the difference of the axial stress in each element with the progress of failure can not be so diminished by the decrease of μ.

In each element, one of the principal stresses is σ_θ (tangential stress), and the others are on the rz-plane. Apart from the specimen ends, the directions of the two principal stresses approximately coincide with the z- and r-axes, and they can written by σ_z and σ_r without large error. σ_z is always the maximum principal stress. It is determined by the position of the element in the specimen, end condition and the degree of progress of failure whether σ_r or σ_θ is the minimum principal stress.

Generally, in short specimens σ_r is compressive throughout the specimen because of end restraint. In long specimens it is tensile in the central region and compression in both ends at first, and this tensile stress gradually changes into compressive with the changes of elastic constants due to the progress of failure. On the other hand, generally, σ_θ near the mid-height region is compressive at the inner part and tensile in the outer part. Thus the minimum principal stress of the outer part at the mid-height region is σ_θ especially in considerably fractured specimen. The surface cracks along the generatrics observed in uniaxially compressed cylindrical specimen with fixed end may be explained that they are caused by this tensile principal stress σ_θ.

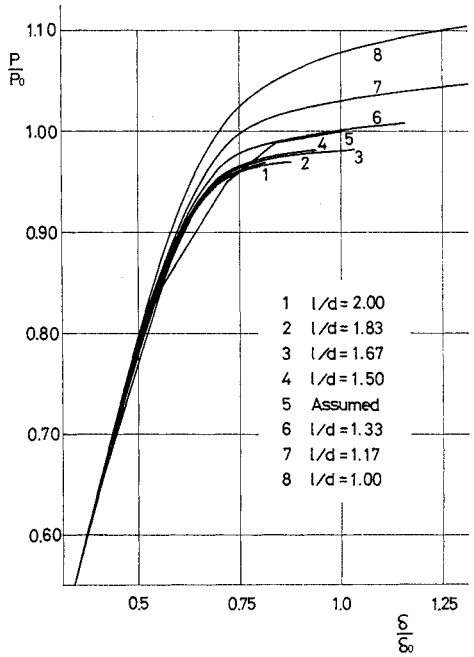

Fig. 11 Effects of end constraint on the apparent stress-strain curves of the specimens compressed between rigid rough platens.

(3) Strength of the specimen

The effects of end restraint on the apparent stress-strain curves of the specimens with various length to diameter ratios compressed between rigid rough platens are shown in Fig. 11. In the early stage of loading the calculated curves are higher than the assumed curve in the numerical analysis. This is previously reported in detail[8], and it is a matter of course from the energetic consideration. In long specimens, they are severely lowered from the assumed curve. In short specimens, they become more and more higher. In order to estimate the strength of the specimen, the strength failure is defined as that occurs when the ultimately fractured elements continuously and transversely cross the specimen. This definition is also adopted by Kajita and Kawamoto.[9] The strength failure of specimen in uniaxial compression test is brought about with the lack of stability caused by the propagation of fracture in the specimen. It is difficult to define the strength failure in the numerical analysis. This is the reason why the above mentioned definition is employed. The relations between the strength and the height-to-diameter ratio of the specimens with fixed end are shown in Fig. 12, in which the open circles indicate the calculated values. This figure shows that the lowest uniaxial compressive strength is about 97% of the assumed uniaxial strength when $l/d=2.0$. The strength increases slightly with the increase of l/d. With the decrease of l/d, especially less than 1.5, apparent uniaxial strength increases severely. Kesler[10] reported the change of uniaxial strength of concrete specimens with various l/d, and obtained the correction factor refered to $l/d=2.0$ for several cases of l/d (Fig. 13). These results are adequately explained by the results of the present numerical analysis.

In the next, it will be discussed the reason why

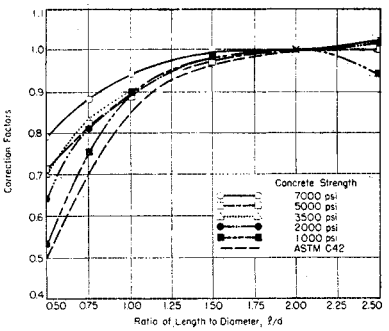

Fig. 13 Correction factors for normal weight, air entrained concretes 6-in diameter specimens (Kesler[10]).

the uniaxial compressive strength of the specimen compressed between rigid rough platens is lower than the ideal uniaxial strength. The elements at the central section of the specimen with height-to-diameter ratio 2.0 are considered. In the early stage of loading, the minimum principal stress is tensile and 0.3~0.5% of the maximum compressive stress. When the fracture initiates in the element near the central section, the value of the maximum principal stress is lower than that of ideally uniaxially compressed specimen. At the central section, the radial tensile stress gradually changes into compressive, and the tangential tensile stress remains in tension especially in the outer part, as previously discussed. According to the adopted fracture condition, the fracture proceeds rapidly in this region and the resulting uniaxial compressive strength with fixed end may be lower than that with fully lubricated. The fracture condition may be considered appropriate judging from the shape of failure surface.

However, in rock-like materials, it is noted that the growth of anisotropy in the course of the ini-

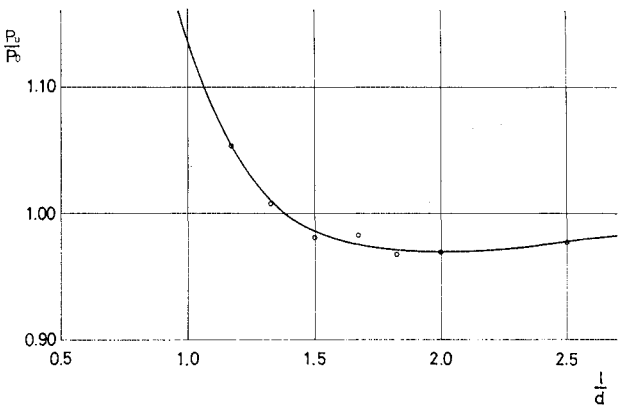

Fig. 12 The relations between the strength and the height-to-diameter ratio of the specimen.

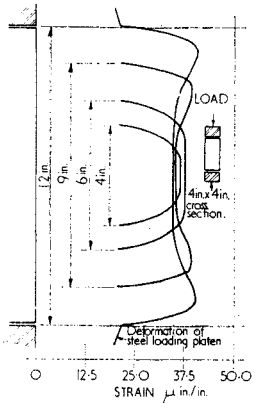

Fig. 14 Variation of lateral deformation profile with height of prism specimen (Newman and Lachance[11]).

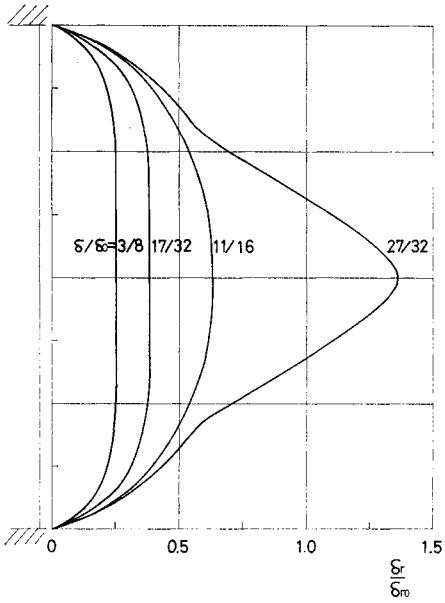

Fig. 15 Variation of lateral deformation profile with height of the specimen with $1/d$ =2.0 and fixed at ends.

tiation and propagation of internal cracks may not be neglected, and that the above conclusion may not be fully supported. When the material elements are approximately assumed to behave macroscopically, it can be concluded that there is a possibility to make the uniaxial strength of a long specimen with fixed ends more or less lower than that of ideally uniaxially compressed specimens.

Kajita and Kawamoto concluded that the calculated strength can be coincide with the experimental

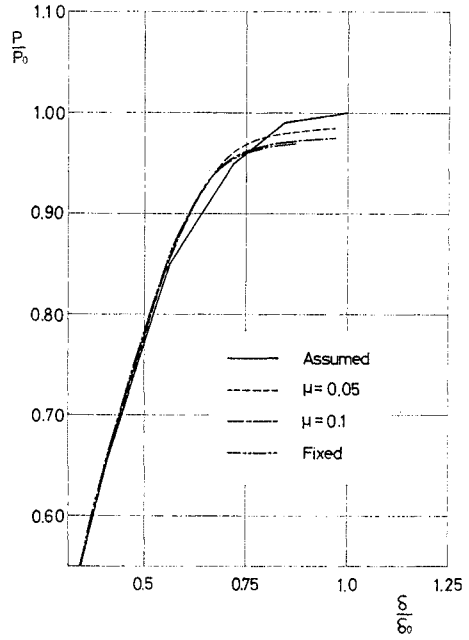

b) $1/d$=1.5

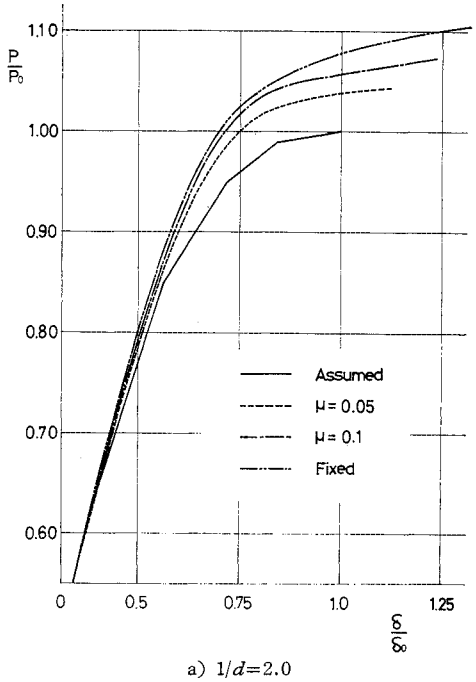

a) $1/d$=2.0

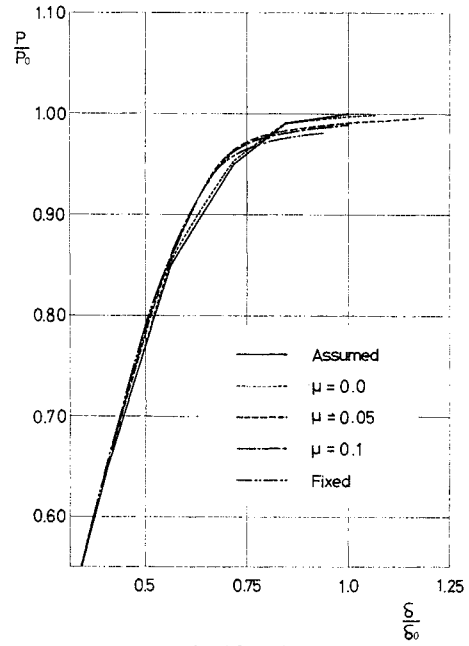

c) $1/d$=1.0

Fig. 16 Apparent stress-strain relations of specimens with several height-to-diameter ratios and with coefficients of end friction.

value by the choice of suitable failure condition. The effect of the end restraint on the uniaxial compressive strength can not be concluded from their discussion, because their results are not compared with the true uniaxial compressive strength of msaterials.

It is recognized by other stress analyses that the tensile radial stress generates in the central parts of the long specimen with fixed end. It is interesting to discuss the deformation of the specimen by considering this tensile stress. The generation of tensile radial stress in this region means that the radial displacement of the specimen is smaller than that of adjacent region. Thus, the cylindrical specimen becomes doubly bulged. Newman and Lachance[11] uniaxially compressed rectangular block specimens with various heights and showed the lateral deformations (Fig. 14). The results show clearly the double bulge. In Seldenrath and Gramberg's experiment[12], however, the double bulge can not be recognized. In authors' analysis the slight double bulge is observed. Although the lateral deformation shows the double bulge, the displacement of the specimen side in the central half height is almost uniform. It may be difficult to detect the double bulge in the uniaxial compression test of rock-like materials. Fig. 15 shows the side displacements of the specimen with $1/d=2.0$ and end fixed at several loading stages. The lateral displacements are fairly uniform in early stage of loading. The central region greatly expands as fracture progresses.

The apparent stress-strain relations of specimens with several height-to-diameter ratios and with several coefficients of end friction are shown in Fig. 16. As previously noted, the mode of fracture approaches uniform with the decrease of the coefficient of end friction. When $1/d=1.0$, the apparent strength decreases with the decrease of the coefficient of end friction and it approaches to the assumed uniaxial compressive strength. On the other hand, when $1/d=1.5$ or 2.0, the apparent strenght increases with the decrease of the coefficient of end friction. The apparent stress-strain curves with the coefficient of end friction $\mu=0.1$ and 0.05 are considerably different from the assumed stress-strain curve of the model material. This results show that the effect of end restraint on the behavior of the specimen is very large.

In Fig. 16(b) the calculated result with $\mu=0.0$ is shown in order to make clear the accuracy of the numerical analysis. Although the calculated result deviates slightly from the assumed one, it may be said that the accuracy is enough.

(4) The influence of Poisson's ratio

In order to make clear the effect of the changes of the Poisson's ratio on the behavior of the specimen, two cases of the increase of Poisson's ratio are assumed as shown in Fig. 17 (Case B, Case C). The calculated stress-strain relations are shown in Fig. 18. In this case, $1/d=1.17$ and $\mu=\infty$ were used. From Fig. 18, it can be concluded that the failure progress is greatly affected by the change of Poisson's ratio.

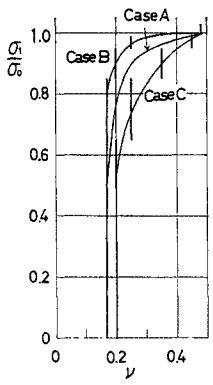

Fig. 17 Assumed three kinds of increase of Poisson's ratio.

4. CONCLUSION

The followings may be concluded :

1) The progress of failure in the compressed specimen is greatly affected by the end restraint. Although the progress of failure is considerably uniform near the central section in long specimen (for instance, length to diameter radio $1/d=2.0$), it is faster in the outer part than in the inner part even near the central section in the short specimen (for instance $1/d=1.0$).

2) The stress distribution in the specimen changes with the progress of failure. With the progress of failure, the axial stress near the central part becomes higher in the inner part. This tendency is

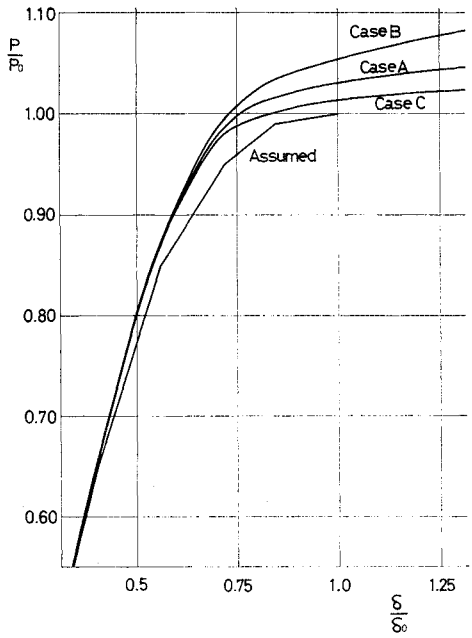

Fig. 18 Apparent stress-strain relations correspond to the increases of Poisson's ratio.

evident when $l/d=1.0$. In the outer part in the central section of the specimen, the hoop stress becomes tensile with the progress of the failure, and this is the minimum principal stress at this region. This stress initiates the cracks along the generatrics at the surface of the uniaxially compressed specimens.

3) The progress of the failure the specimen and the stress distribution in the specimen approaches to the uniform state with the decrease of the coefficient of end friction. Even when the coefficient of end friction is 0.05, the behavior of the specimen is affected by the end restraint and it is considerably different from the ideal one.

4) When the material elements can be supposed to behave macroscopically, the uniaxial compressive strength of the specimen is affected by the end restraint. In the present analysis, the uniaxial strength of end fixed specimen with $l/d=2.0$ is about 97% of the ideal uniaxial compressive strength. As l/d decreases from 1.5, enormous increase of the apparent strength was observed. The more the coefficient of end friction is reduced, the more the apparent uniaxial strength of the specimen approaches to the ideal strength.

REFERENCES

1) Niwa, Y., S. Kobayashi and A. Miyaji : "Some Considerations on Fracture Criteria of Cement Mortar Subjected to Multiaxial Compression", Review of the 23rd General Meeting of the Cement Association, Japan, 1969, pp. 163-168.
2) Niwa, Y., W. Koyanagi and K. Nakagawa : "Failure Processes of Concrete under Triaxial Compressive Stress", Proc. JSCE, No. 185, Jan. 1971, pp. 31-41 (in Japanese)
3) Vile, G.W. : "The strength of concrete under short term static biaxial stress", Proc., International Conference on the Structure of Concrete, London, Sept. 1965, Cement and Concrete Association 1968, pp. 275-288.
4) McCreath, D.R., J.B. Newman and K. Newman : "The influence of aggregate particles on the local strain distribution and fracture mechanism of cement paste during shrinkage and loading to failure", Materiaux et Construction, Vol. 2, No. 7, 1969, pp. 73-85.
5) *ibid* 1)
6) Niwa, Y., S. Kobayashi and K. Nakagawa : "The Influence of End Frictions on Stresses in Compressed Specimens", Memo. Faculty of Eng., Kyoto Univ., Vol. 31, Jan. 1969, pp. 1-11.
7) Niwa, Y. and S. Kobayashi : "Failure Criterion of Cement Mortar under Triaxial Compession", Memo. Faculty of Eng., Kyoto Univ., Vol. 29, Jan. 1967, pp. 1-15.
8) Niwa, Y., S. Kobayashi and K. Nakagawa : "The Influence of End Friction and Poisson's Ratio on Stresses in Compressed Specimens", J. Soc. Materials Science, Japan, Vol. 19, No. 196, 1970, pp. 63-69 (in Japanese).
9) Kajita, T. and T. Kawamoto : "Finite Element Analysis of Uniaxial Compressive Strength of Cylindrical Brittle Specimen", Proc. JSCE, No. 177, May 1970, pp. 71-76 (in Japanese).
10) Kesler, C.E. : "Effect of Length to Diameter Ratio on Compressive Strength—An ASTM Cooperative Investigation", Proc. ASTM, Vol. 59, 1959, pp. 1216-1228.
11) Newman, K. and L. Lachance : "The Testing of Brittle Materials under Uniform Uniaxial Compressive Stress", Proc., ASTM, Vol. 64, 1964, pp. 1044-1067
12) Seldenrath, Th.R. and J. Gramberg : "Stress-Strain Relations and Breakage of Rocks", Mechanical Properties of Non-Metallic Brittle Materials, (W.H. Walton, Ed.) pp. 29-105, Butterworth, London, 1958.

(Recived April 19, 1971)